

# Value-Based Deep Learning Acceleration

Andreas Moshovos, Jorge Albericio\*, Patrick Judd, Alberto Delmás Lascorz,  
Sayeh Sharify, Tayler Hetherington†, Tor Aamodt†, Natalie Enright Jerger  
University of Toronto, \*NVIDIA, †University of British Columbia

## ABSTRACT

This article summarizes our recent work on *value-based* hardware accelerators for image classification using Deep Convolutional Neural Networks (CNNs). The presented designs exploit runtime value properties and that are difficult or impossible to discern in advance. These include values that are zero or near zero and that prove ineffectual, reduced yet variable precision needs, or ineffectual bits in values. The designs offer a spectrum of choices in terms of area cost, energy efficiency and relative performance covering embedded to server class installations.

## 1. INTRODUCTION

A few years ago the idea of computing systems that can converse with us or drive cars seemed the stuff of fiction. Yet today, computing systems are learning to “see”, “hear”, “read”, “write” and, in general, interact with the physical world in ways we typically associate with intelligent beings. The technology that drives these advances is Machine Learning with much of the recent success due to Deep Learning (DL). While conventional programs have to be meticulously constructed to anticipate any possible scenario, often an impossible task, DL “learns” by example or by trial and error.

The foundations of DL date back to the 1950s with many innovations introduced since then. However, it is only in recent years that DL has become practical due to the confluence of three factors: 1) DL algorithmic innovations, 2) the availability of vast amounts of computerized data to learn from, and 3) the advent of sufficiently powerful hardware. These recent DL successes have fueled efforts for broadening the scope and sophistication of DL applications. However, further innovation in DL greatly depends on computing hardware systems with even greater computational power. In the past decades, hardware performance advances were possible at regular intervals primarily because semiconductor technology scaling enabled us to build hardware with more and faster transistors for the same or less cost. Unfortunately, this is no longer true due to power constraints [8].

A viable way to sustain these much needed performance advances is via hardware accelerators. A hardware accelerator is designed to excel at the processing of a specific algorithm or class of algorithms. It sacrifices generality for greater energy efficiency and performance. Accelerators have been extremely successful in various application domains such as computer graphics or communications where performance

improvements of three orders of magnitude are routinely possible. We believe that DL applications can similarly benefit and have been designing such accelerators targeting DL applications.

In particular, we focus on a core component of a DL system, *image classification* which identifies various objects in an image frame, that is in a 2D projection of the physical world as acquired by an imaging sensor. The building blocks used for this DL application are very similar and often identical to those used for other DL applications. Accordingly, techniques developed for accelerating image classification should be broadly applicable. For example, an application area where DL is a key enabling technology and where the needs for higher data storage and processing capacity is evident is autonomous driving (AD), e.g., [3]. Many components of a complete AD system use DL. This article focuses on using DL to detect objects around the vehicle, a key piece of information needed for navigation.

This article summarizes our recent work on *value-based* hardware accelerators for image classification using Deep Convolutional Neural Networks (CNNs). Section 2 provides background on CNNs, while Section 3 introduces acceleration concepts, presents a state-of-the-art structure-based CNN accelerator and motivates our value-based approach. Sections 4 through 6 explain three different value properties and the corresponding value-based accelerator designs. Finally, Section 7 comments on informational inefficiency that underlies our and many other DL acceleration approaches.

## 2. CONVOLUTIONAL NEURAL NETWORKS

Figure 1a shows that a CNN is a software pipeline of *layers*. An input, which is typically a 2D image, is fed into the first layer. The image is treated as a 3D array comprising three 2D images one per red, blue, and green color plane. Each value is an *activation* and the purpose of the CNN is to *infer* what type of object these activations represent. In its simplest form, the CNN outputs a vector of probabilities with one element per possible object class. This approach can be extended to detect the position of multiple objects or even the trajectory of objects given a sequence of frames. As the figure shows, the output can be an annotated image with bounding boxes identifying various objects of interest such as other vehicles, pedestrians, and street signs.

While there often many layers, hence the term *Deep Learning*, there are only a few layer types. In image classification the *convolutional* layers (CVLs) account for more than 90%

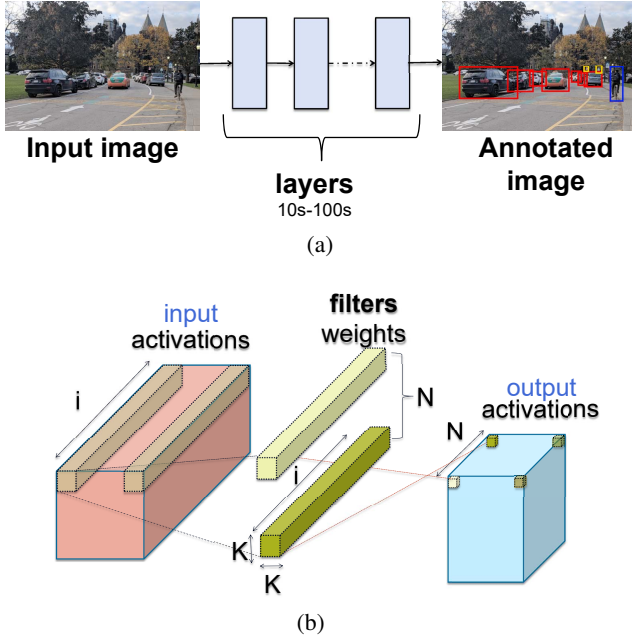


Figure 1: a) A CNN. b) A Convolutional Layer.

of the execution time on modern graphics processors, the current commodity architecture of choice for CNNs. Fully-connected layers (FCLs), a specialized form of CVLs, account for most of the remaining time.

Informally, each CVL applies several filters to the 3D input activation array producing a 3D output activation array (shown in Figure 1b). Each output activation is the result of an inner-product of a filter and an equally-sized subarray of the input activation array. The filters are 3D arrays of *weights* which are pre-determined values that contain the network’s “knowledge”. The weights are determined during an earlier training phase where the network, starting from randomly selected weight values, is trained by processing several pre-annotated example images. A typical CVL performs hundreds of inner products, each comprising hundreds to thousands activation and weight pairs.

Formally, a CVL processes and produces 3D activation arrays of real numbers. The layer applies  $N_f$  3D filters in a sliding window fashion using a constant stride  $S$  to produce an output 3D array. The input array contains  $N_x \times N_y \times N_i$  activations. Each of the  $N_f$  filters, contains  $K_x \times K_y \times N_i$  real-valued weights. The output activation array dimensions are  $O_x \times O_y \times N_f$ , that is its depth equals the filter count. Each filter corresponds to a desired *feature* and the goal of the layer is to determine where in the input activation array these features appear. Accordingly, each constituent 2D array along the  $n$  dimension of the output activation array corresponds to a *feature*. The layer computes the inner product of a filter and a *window*, a filter-sized, or  $K_x \times K_y \times N_i$  sub-array of the input activation array. The inner product is then passed through an *activation function*, such as the *Rectifier Linear Unit* (ReLU) producing an output activation. If  $a(y, x, i)$  and  $o(y, x, i)$  are respectively input and output activations,  $w^f(x, y, i)$  are the weights of filter  $f$  and  $R$  is the activation function. The output

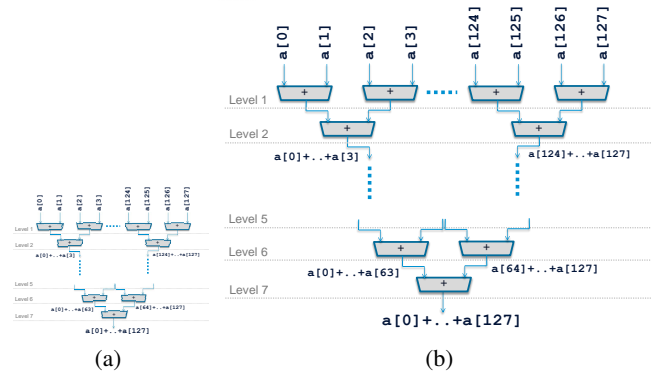


Figure 2: Adding 128 numbers: a) Machine code implementation, and b) Structure-based hardware accelerator.

activation at position  $(x', y', n)$  is given by:

$$o(y', x', f) = R \left( \underbrace{\sum_{x=0}^{K_x-1} \sum_{y=0}^{K_y-1} \sum_{i=0}^{N_i-1} w^f(x, y, i)}_{\text{window}} \times \underbrace{a(x+x' \times S, y+y' \times S, i)}_{\text{input activation}} \right)$$

output activation

The layer applies filters repeatedly over different windows positioned along the X and Y dimensions with stride  $S$ , and there is one output activation per window and filter. Accordingly, the output activation array dimensions are  $O_x = (N_x - K_x)/S + 1$ ,  $O_y = (N_y - K_y)/S + 1$ , and  $O_i = N_f$ . A fully-connected layer can be implemented as a CVL where the filter dimensions match those of the input activation array.

For clarity, in what follows the term **brick** refers to a set of 16 elements of a 3D activation or filter array which are contiguous along the  $i$  dimension, e.g.,  $n(x, y, i) \dots n(x, y, i + 15)$ . Bricks will be denoted by their origin element with a  $B$  subscript, e.g.,  $n_B(x, y, i)$ .

### 3. ACCELERATION PRIMER

Being able to process CNNs faster can yield multiple benefits for future ADs: 1) it enables processing higher resolution frames, 2) it enables processing multiple imaging sources, and 3) reduces reaction times. As power has become the limiting factor in modern hardware, further boosting of processing speed requires improving energy efficiency, that is reducing the amount of energy expended to perform each computation.

Therein lies the great opportunity for hardware accelerators. Specifically, existing computing hardware is often general purpose in that it is designed to perform relatively well for numerous applications. Unfortunately, with generality comes inefficiency. For example, consider the simple task of *reducing*, that is adding 128 numbers, a subcomputation of an output activation calculation. We should be able to just read these 128 numbers and add them together. However, conventional processors perform a lot more work to achieve the same effect. As Figure 2a shows, a conventional processor implements this reduction using a loop of several *instructions*. Executing an instruction entails several actions: reading the

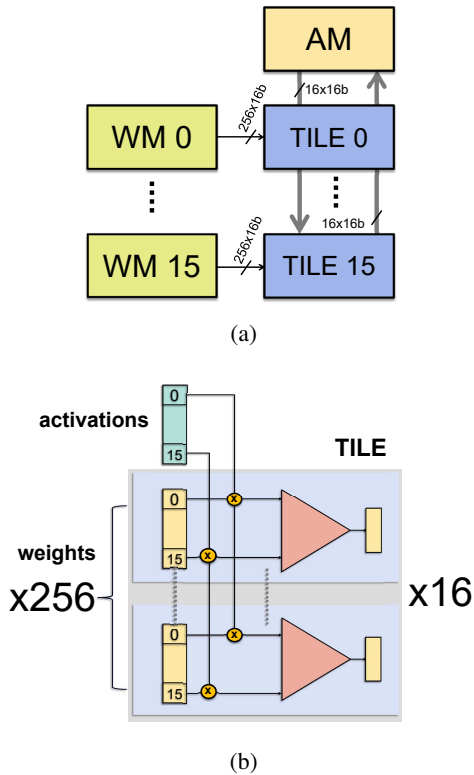


Figure 3: a) DaDianNao Overview. b) DaDianNao Tile.

instruction representation from memory; decoding it into a set of actions; reading the source data operands; performing a calculation; writing the result; and figuring out which instruction to execute next. To reduce 128 values, a processor executes 643 instructions and performs 643 and 128 memory reads for the instructions and the data inputs, respectively.

Specialized reduction hardware could instead simply use an adder tree as Figure 2b shows. It would perform just 128 data reads, and 128 additions organized in 7 level/steps, reducing the processing steps by  $9\times$ . This is an example of a *computation structure-based* accelerator.

The accelerators described in this work go beyond this conventional approach to acceleration by relying also on data content. Examining data content opens up new opportunities for acceleration. For example, what if roughly 50% of our numbers are zero but we do not know in advance which ones. Could we build a better accelerator?

### 3.1 A Structure-Based CNN Accelerator

An example of a state-of-the-art accelerator that relies on the computation structure of neural networks is *DaDianNao* (*DaDN*) [4]. As Figure 3a shows, a *DaDN* chip comprises 16 processing tiles each with its own slice of 2MB eDRAM *Weight Memory* (WM), and a central 4MB eDRAM *Activation Memory* (AM). Each tile contains 16 *Inner Product units* (IPUs) each containing 16 multipliers and an adder tree to compute the inner product of a weight and an activation brick each cycle. Each cycle an input activation brick is broadcast from AM to all IPUs, while each IPU fetches a different weight brick. In total, a tile processes 256 weights, and 16

activations per cycle. Larger inner products are computed over multiple cycles and finally are passed through an activation function,  $R$ , to produce an output activation. Each cycle, the whole chip processes 16 activations and  $256 \times 16 = 4K$  weights producing  $16 \times 16 = 256$  partial sums. Processing starts by reading from external memory the first layer’s filter weights, and the input image. The weights are distributed over the WMs and the input is stored into AM. While the current layer is being processed, the weights for the next layer can be loaded from off-chip. *DaDN* is a structure-based accelerator since it implements the layer computations as-is regardless of the actual values being computed.

The discussion that follows uses *DaDN* as the baseline design, however, the techniques described are applicable to other accelerator organizations as well. Since *DaDN* is a massively data-parallel design, our implementations also target this design style. Specifically, two important properties that we wish to maintain are: 1) wide, regular accesses to the various memories, and 2) regular computations across all tiles and inner-product units. The first property maintains high utilization of precious on- and off-chip memory bandwidth, while the second allows the use a common control unit and thus avoids the cost of many little independently operating processing units.

### 3.2 Our Approach

We mirror the design philosophy that yielded many successful techniques for improving performance for modern general-purpose cores which exploit the *expected* behavior of programs; programs do not behave randomly but rather tend to exhibit specific idiosyncratic behaviors. A well-known example is biased branches which branch predictors exploit. Accordingly, we target identifying properties in the value stream of CNNs. Additional opportunities exist by co-designing the CNN software and hardware. However, *not requiring* any modifications to the CNN results in immediate benefits and reduces the burden on the CNN designers.

### 3.3 Methodology

All systems are modelled using the same methodology for consistency. A custom cycle-accurate simulator models execution time. Computation is scheduled such that all designs see the same reuse of weights. To estimate power and area, all tile pipeline designs are synthesized with the Synopsys Design Compiler for a TSMC 65nm library and laid out with Cadence Encounter. Circuit activity is captured with ModelSim and fed into Encounter for power estimation. All SRAM buffers are modelled using *CACTI* while the eDRAM area and energy are modelled with *Destiny*.

### 3.4 Overview

Table 1 summarizes our various designs and reports their relative performance, energy efficiency and area normalized to *DaDN*. The sections that follow describe each of these designs in more detail.

## 4. INEFFECTUAL ACTIVATIONS

Our first observation is that many activations turn out to be zero at run-time, and even more are close enough to zero that they can be treated as if they are zero. In either case,

**Table 1: Value-Based Accelerator Characteristics Relative to *DaDN* [4]. Reported is the performance, energy efficiency and area compared to an equivalent *DaDianNao* configuration shown under column “*DaDN Conf.*”. *DaDN* configurations are labelled as “*Tiles - Filters/Tile - Products/Filter*”.**

Accelerator	Configuration	Performance	Power	Area	Frequency	Tech. Node
<i>DaDianNao (DaDN)</i> [4]	16-16-16	3.9 Tmul/sec	17.6 Watt	78mm <sup>2</sup>	980 Mhz	65nm
Accelerator	Compared to <i>DaDN Conf.</i>	Relative Performance	Relative Energy Efficiency	Relative Area	Layers	Value Property
<i>Cnvlutin</i> [2]	16-16-16	1.6×	1.47×	1.05×	CVL	Ineffectual Activation Values
<i>Stripes</i> [13]	16-16-16	1.9×	1.14×	1.32×	CVL	Per Layer Activation Precision
<i>Tartan</i> [7]	16-16-16	1.9× (CVL) 1.6× (FCL)	1.18× (CVL) 1.06× (FCL)	1.49×	CVL+FCL	Per Layer Activation+Weight Precision
<i>Dynamic Stripes</i> [6]	16-16-16	2.6×	1.54×	1.35×	CVL	Dynamic Activation Precision
<i>Loom</i> [16]	1-8-16	2.85× (CVL) 1.85× (FCL)	2.22× (CVL) 1.51× (FCL)	1.14×	CVL+FCL	Dynamic Activation and Per Layer Weight Precision
<i>Pragmatic</i> [1]	16-16-16	4.3×	1.71×	1.68×	CVL	Ineffectual Activation Bits

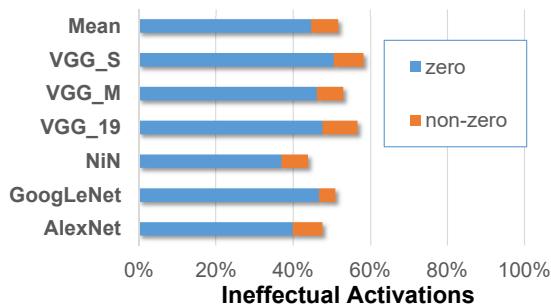


**Figure 4: Average fraction of convolutional layer multiplication input activations that prove ineffectual.**

the energy of the transfers of these *ineffectual* activations and of the corresponding multiplications and additions can be straightforwardly avoided by temporarily “powering off” the respective links and compute units. While this approach reduces energy, it does not improve performance. What if we could completely eliminate these actions and process in their place some of the other *effectual* activations?

Figure 4 reports the average total fraction of activation inputs to multiplications that prove ineffectual across all convolutional layers and across all inputs. On average 44% of all activations are zero. An additional 7% of activations can be ignored as well without affecting accuracy (TOP-1). The position of these ineffectual activations depends on the input data values, and hence it would be challenging for a static approach to eliminate the corresponding computations.

But why would a network produce so many zero activations? The answer lies in the nature and structure of CNNs. At a high level it is convenient to think that CNNs are designed so that each CNN layer attempts to determine whether and where the input contains certain learned “features” such as lines, curves or more elaborate constructs. The presence of a feature is encoded as a positive-valued activation output and the absence as a zero-valued activation output. It stands

to reason that when features exist, most likely they will not appear all over the input, moreover, not all features will exist. CNNs detect the presence of features using the CVLs to produce an output encoding the likelihood that a feature exists at a particular position as a number. Negative values suggest that a feature is not present. CVLs are immediately followed by a ReLU layer that clamps negative values to zero.

#### 4.1 The *Cnvlutin* Accelerator

Modifying *DaDN* so that it can seamlessly avoid ineffectual activations is a challenge. When processing all activations, wide accesses to both AM and WM are trivially possible. Moreover, the positions of activation and their corresponding weights are known well in advance and are independent of their values. The straightforward approach to “skipping” the ineffectual activations is of no use: by the time activations are fetched from AM, there is not enough time to test their values and to selectively fetch additional activations and weights to replace those that are ineffectual; not only would this require several narrow AM and WM accesses, but also several attempts may be required to find a set of 16 effectual activations that can be processed in parallel by all tiles. By that time, the base design that does not attempt to skip ineffectual activations would be further ahead. Often “dumb but fast” hardware is hard to beat.

The simplified example of Figure 5a illustrates the solution used by our *Cnvlutin* (CNV) accelerator. The example shows a simplified *DaDN* accelerator with two inner product units, each processing four activation and weight pairs per cycle. This *DaDN* needs 4 cycles in total to process the 16 products necessary and to produce the two output activations corresponding to filters F0 and F1.

Figure 5b shows how the equivalent simplified CNV design needs only two cycles. Activations are now augmented with relative offsets. For example, a 4-activation brick containing (1, 0, 4, 0) is encoded as ((1, 0), (4, 2), (0, 0), (0, 0)) where the (4, 2) pair indicates that in the original activation array, 4 was at offset 2 within the brick. CNV decouples the activation lanes allowing them to proceed independently. By using the

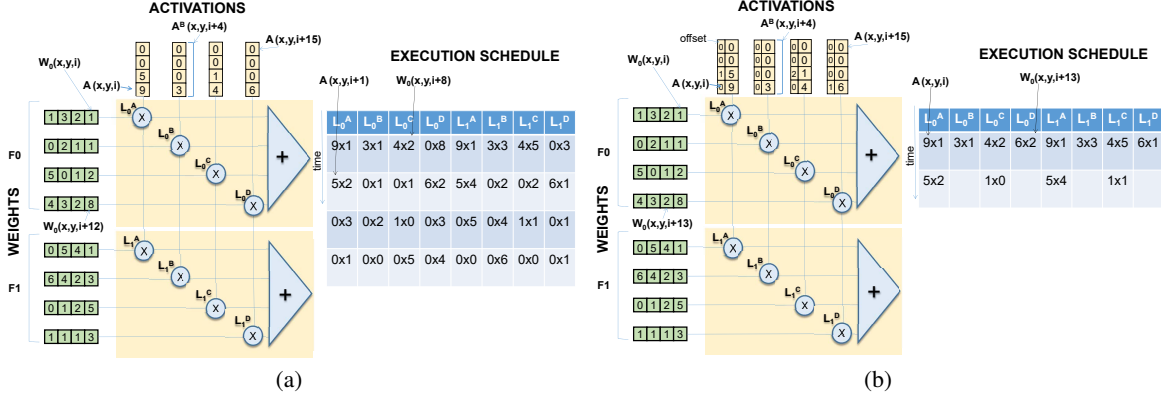


Figure 5: a) *DaDN* processes all activations, while b) *Cnvlutin* processes only non-zero activations.

offset, the tiles can fetch the corresponding weight from the WM maintaining wide accesses (one activation corresponds to 256 weights in *DaDN*).

However, how are the offsets generated and the activation values neatly packed into the bricks so that the effectual activations appear first thus avoiding many narrow AM accesses? Except for the first layer, the input activation array to each layer is the output activation array of the immediately preceding layer. Moreover, several tens to hundreds of cycles are needed to generate each output activation, given existing layer dimensions. Accordingly, there is plenty of time to encode activations in the desired format while generating them. Albericio *et al.* describe the process in more detail [2] but several alternatives exist.

## 5. PRECISION

Conventional general purpose hardware and many accelerators support one or a few precisions for numerical values. For example, *DaDN* uses 16-bit fixed-point values. However, the precision required by CNNs varies significantly not only across networks but also across the layers of the same network [12]. However, since most existing implementations rely on a *one-size-fits-all* approach, they use the *worst-case* numerical precision for all values and cannot benefit from the variable precision requirements of CNNs.

*Stripes (STR)* allows per-layer precision activation selection providing a new dimension upon which to improve performance [13]. To do so, *STR*'s execution units are designed so that execution time scales linearly with the length in *bits* of the numerical precision needed by each layer. Compared to *DaDN* that uses a 16-bit fixed-point representation, *STR* would ideally improve performance at each layer by  $16/p^L$  where  $p^L$  is the layer's required precision length in bits.

Before we touch upon the key design decisions in *STR*, Table 2 reports the *precision profile* per network, which is the set of the per-layer fixed-point representation lengths needed for *activations* to maintain the network's classification accuracy [12]. For each network, the per layer precisions are shown separated with dashes. Overall, the precision needed varies from as much as 14 bits (layer 1, GoogLeNet) to as little as 5 bits (layer 3, AlexNet). The *Ideal Speedup* column reports the speed that is possible over *DaDN* if performance

Table 2: Per Convolutional layer activation precision profiles needed to maintain the same *top-1* accuracy as in the baseline (100%) *Ideal: Potential speedup with Stripes.*

Network	Per Layer Activation Precision in Bits	Ideal Speedup
AlexNet	9-8-5-5-7	2.38
NiN	8-8-8-9-7-8-8-9-9-8-8-8	1.91
GoogLeNet	10-8-10-9-8-10-9-8-9-10-7	1.76
VGG_M	7-7-7-8-7	2.23
VGG_S	7-8-9-7-9	2.04
VGG_19	12-12-12-11-12-10-11-11-13-12-13-13-13-13-13	1.35

scales by  $16/p^L$  where  $p^L$  the precision used. *Proteus* takes advantage of this precision variability to reduce off-chip memory traffic by storing and transferring only as many bits as necessary [11].

### 5.1 Stripes' Approach

Figure 6a shows a simplified *DaDN* IP block computing the inner product of vectors  $(A_0, A_1)$  (activations) and  $(B_0, B_1)$  (weights), where all values are encoded using 2 bits of precision and are shown in binary. The IP uses bit-parallel multipliers and in a single cycle computes the pairwise element products of  $A$  and  $B$ ,  $(1 \times 1, 0 \times 3)$ , or  $(1, 0)$ . The two products are then added through a bit-parallel adder to calculate the final inner product  $A \cdot B = (1)$  which is then truncated to 2-bits. In total, the input bandwidth of this unit is 8 bits per cycle (2 activations of 2 bits per cycle and 2 weights of 2 bits per cycle), and its output bandwidth is 2 bits per cycle.

Figure 6b shows *STR*'s approach where  $A$ 's values have been transposed and are now processed bit-serially over two cycles. However, since the upper bits of  $A_0$  and  $A_1$  are both zero, both can be represented in just one bit of precision. Hence, one cycle is sufficient to calculate the inner product. In general, execution time now becomes proportional to the bit-width of  $A$ 's values and as long as there is enough precision in the partial output buffer and the adders, a range of  $A$  precisions can be naturally supported.

However, as described the unit of Figure 6b would at best match the performance of *DaDN*; if both bits of precision

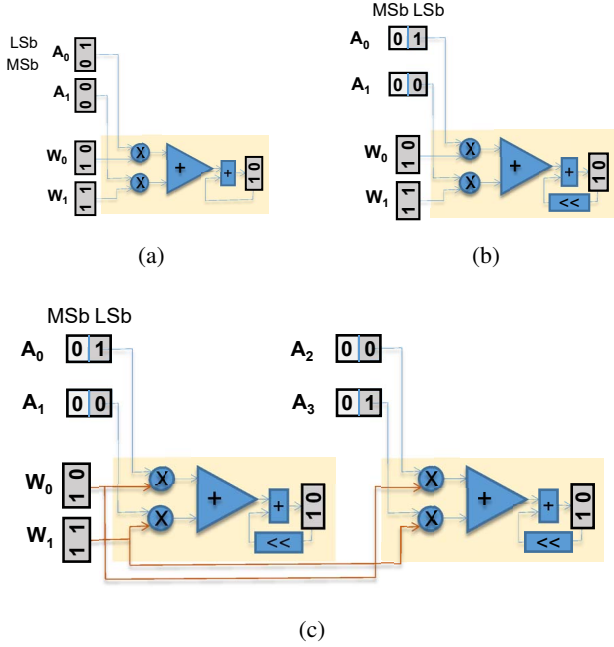


**Figure 6: Exploiting Precision to Boost Performance (a) Bit-Parallel Computation: (b) Bit-serial computation for  $A_x$ : Execution time depends on  $A_x$ 's precision. (c) Bit-serial computation for more activations matching (a)'s throughput. The same weights are used for both pairs of activations.**

are needed, it will be twice as slow. Fortunately, there is abundant parallelism in the CVLs which *STR* exploits to offer at least the same computational bandwidth as the bit-parallel design. As Figure 6c shows, *STR* could process another pair of activations  $A'$  in parallel as long as the inner product  $A' \cdot B$  is also needed. In the worst case, this unit would produce two inner products every two cycles matching *DaDN*'s throughput. In the best case, it will need just one cycle, twice as fast as *DaDN*.

In our example, two additional activations were sufficient to always match the performance of *DaDN* since we assumed that activations used up to 2 bits of precision. Since *DaDN* uses 16 bits of precision, *STR* needs to process 16 times as many activations in parallel. Figure 7a shows a portion of an *STR* tile that replaces a single *DaDN* IP and that uses exactly the same number of external connections. Instead of using the 256 activation wires to communicate 16 16-bit activations, *STR* communicates 1 bit from each of 256 activations. Whereas *DaDN* had one IP multiplying 16 pairs of 16-bit activations and weights, *STR* has 16 serial inner product units (SIPs), each multiplying 16 pairs of a 16-bit weight and a single-bit activation. Whereas *DaDN* needed multipliers, *STR* can use AND gates instead. The same set of 16 16-bit weights is used by all 16 SIPs in the row. However, each SIP is given a different set of 16 activations each corresponding to a different window of the input activation array as Figure 7b shows.

## 5.2 Dynamic Precision

*STR* relies on profile-derived precisions per layer. However, in practice these precisions will probably exceed those necessary for two reasons: 1) the precisions are meant to be sufficient for *any* possible input, and 2) the precisions are for the full layer. Given a specific input image, it stands to reason that the precisions needed may be narrower. Moreover, at any given point of time, *STR* processes only 256 activations in parallel. The precision needed to represent these 256 specific values will most likely be narrower than that needed to represent all activations for the layer. Dynamic Stripes extends *STR* to trim precisions on-the-fly and at every cycle by adjusting to the set of activations that are being processed concurrently.

## 5.3 Fully-Connected Layers

It is possible at an additional area cost to achieve performance improvements for FCLs as well. *STR* cannot improve performance for FCLs since they only contain one window and thus at least 16 cycles are needed to load a different set of weights per SIP. As a result, it always takes 16 cycles to process a set of activations and weights regardless of the precision used for the activations. The TARTAN extension to *STR* takes advantage of the variable precision requirements for weights [7]. In TARTAN, performance for FCLs improves by  $\frac{16}{\max(P_a, P_w)}$  where  $P_a$  and  $P_w$  the precisions of the activations and weights respectively. The key insight behind TARTAN is that the 16 wires that are used during CVL processing to broadcast the same weight to all SIPs along the same row can be used to bit-serially load a different weight to each SIP over  $P_w$  cycles for FCLs. The loading of the next set of weights can be overlapped with the processing of the current set.

## 5.4 Exploiting Weight and Activation Precision

So far our designs are capable of exploiting the precision of activations only for CVLs, or of either activations or weights for FCLs (TARTAN). *Loom* takes advantage of the precisions of *both* [16]. In *Loom*, execution time scales with  $\frac{256}{P_w^L \times P_a^L}$  and  $\frac{16}{\max(P_w^L, P_a^L)}$  for CVLs and FCLs, respectively, where  $P_w^L$  and  $P_a^L$  are the weight and activation precisions needed for layer  $L$ . However, *Loom* requires  $256 \times$  the parallelism to guarantee that it will always be as fast as an equivalent *DaDN* configuration. For this reason, it is appropriate for smaller scale designs such as those appropriate for mobile or embedded devices. Still, a configuration that is equivalent to just 1/2 of a tile of *DaDN* can saturate a high bandwidth memory interface offering 512GB/s. Table 1 reports the characteristics for a *Loom* configuration that operates at a single bit granularity. Better energy efficiency is possible when operating at a 4-bit granularity.

## 6. EFFECTUAL BIT CONTENT

The final value property that we exploit is *bit density*, that is the fraction of activation bits that are one. Binary multiplication can be broken down into a summation of single bit multiplications (ANDs). For example,  $a \times w$  is calculated as  $\sum_{i=0}^p a_i \cdot (w \ll i)$ , where  $a_i$  is the  $i$ -th bit of  $a$ . The multiplier computes  $p$  terms, each product of the shifted operand  $w$  and a bit of  $a$ , and adds them to produce the final result. With this

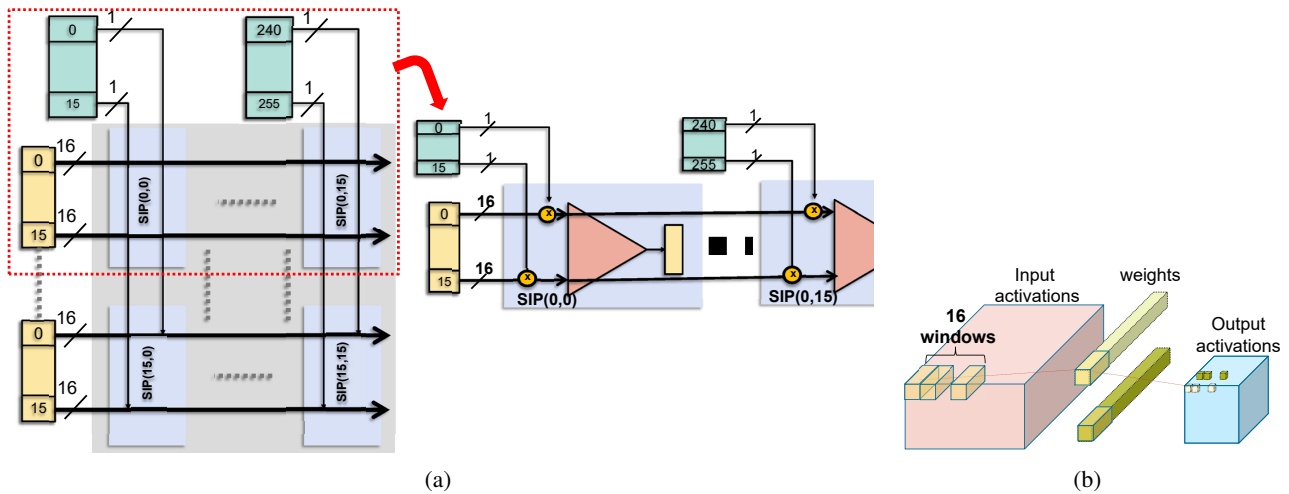


Figure 7: a) Stripes' tile detail. b) Where Stripes finds the parallelism it needs.

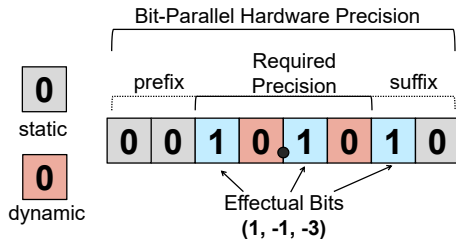


Figure 8: Sources of ineffectual computation with conventional positional representation and fixed-length hardware precision.

in mind, any time an activation bit that is zero is multiplied with a weight it adds nothing to the output activation.

We can categorize these zero bits as either statically or dynamically ineffectual. *Statically* ineffectual bits are those that can be determined to be ineffectual *a priori*. They result from using a data format with more precision than is necessary. In this case, 1's may also be statically ineffectual. Figure 8 shows an example illustrating these ineffectual bits using an 8-bit unsigned fixed-point number with 4 fractional and 4 integer bits. Assume that we know ahead of time that our data only needs 5 bits, then we have 3 statically ineffectual bits as a prefix and suffix to the required precision. While  $10.101_{(2)}$  requires just five bits, two dynamically generated zero bits appear at positions 0 and -2. In total, five ineffectual bits will be processed generating five ineffectual terms. STR and its variants do exploit these statically ineffectual bits. Dynamic Stripes can exploit some of the dynamically ineffectual zero bits as well. No STR variant can exploit the dynamically ineffectual zero bits that appear in between bits that are one.

The non-zero bits can instead be encoded with their corresponding exponents (1,-1,-3). While such a representation may require more bits which is undesirable for storage, dynamically generating them and only computing the non-zero terms may benefit performance and energy efficiency. We show that with the multitude of zero bits and data reuse in CNNs, there is significant potential to improve performance

while reusing hardware to save area.

For the networks studied, only 7.6% and 28% of the activation bits are effectual for the 16-bit fixed-point and 8-bit quantized [17] representations, respectively. These point to a potential performance improvement of  $13\times$  over *DaDN*. Even if we assume that the zero-valued activations can be removed the corresponding fractions of effectual bits remain low at 19% and 41%, respectively.

## 6.1 Pragmatic

*Pragmatic (PRA)* is an accelerator whose goal is to process only the *effectual* (non-zero) bits of the activations. PRA processes the activations bit-serially while compensating for the loss in computation bandwidth by exploiting the abundant parallelism of convolutional layers similar to *STR*. However, *Pragmatic* skips the activation bits that are zero, a task that required the confluence of several design choices and techniques to realize. Albericio *et al.* describe the design in more detail [1].

Configurations of PRA that use less activation lanes per tile are  $7.8\times$  faster than an equivalent *DaDN* configuration.

## 7. CONCLUSION

Hardware acceleration of Deep Learning is an active area of research; unfortunately we cannot fully review this area due to limited space. However, most recent advances exploit various forms of *informational inefficiency* in CNNs and other DNNs.

At the value level, many activations and weights are ineffectual. Han *et al.*, retrain NNs to eliminate ineffectual weights and eliminate computations with zero-valued activations and ineffectual weights [9]. Other work shows that much smaller networks than the originally proposed ones can maintain accuracy [10], suggesting that networks are often over-provisioned. SCNN avoids computations with both ineffectual weights and activations [15]. Recent evidence suggests that for a given storage budget weight pruning large networks offers better accuracy than naively scaling down networks to size [18]. However, the occurrence of ineffectual activations appears to be an intrinsic property of CNNs as

their neurons are designed to detect the presence of relevant features in their input. Combining ineffectual weight skipping with Stripes or Pragmatic offers benefits for all activations and would be interesting to explore further.

Informational inefficiency manifests also in excess of precision which Stripes exploits. Various forms of quantization also exploit this phenomenon e.g., [17] whereas other designs hardwire different per layer precisions [14]. At the extreme end of the spectrum are “binarized” networks [5] that use binary weights and/or activations. Where such networks are possible, they are preferable due to their reduced area, power, and complexity.

In all, the aforementioned body of work suggests that existing networks exhibit informational inefficiency at various levels and for various reasons. Whether these inefficiencies are best exploited statically, dynamically, or both is an open question. Furthermore, which forms of inefficiency will persist as networks evolve remains to be seen.

Our designs work with out-of-the-box NNs thus offering immediate benefits. More importantly, they open up new opportunities and incentives for NN designers, providing a safe path towards innovation while offering rewards for even small advances. For example, Stripes, if deployed, can accelerate innovation in low-precision NN design with an eye towards binary and ternary networks. This is because it enables experimentation with the whole spectrum of precision choices while also delivering excellent performance for full-precision networks. This will incentivize the ML community to further invest in this direction delivering immediate, proportional rewards. Eventually, if extremely low-precision networks take over, more efficient hardware platforms can be deployed.

## 8. REFERENCES

- [1] J. Albericio, A. Delmás, P. Judd, S. Sharify, G. O’Leary, R. Genov, and A. Moshovos, “Bit-pragmatic deep neural network computing,” in *Proceedings of the 50th Annual IEEE/ACM International Symposium on Microarchitecture*, ser. MICRO-50 ’17. New York, NY, USA: ACM, 2017, pp. 382–394. [Online]. Available: <http://doi.acm.org/10.1145/3123939.3123982>
- [2] J. Albericio, P. Judd, T. Hetherington, T. Aamodt, N. Enright Jerger, and A. Moshovos, “Cnvlutin: Ineffectual-neuron-free deep neural network computing,” in *2016 IEEE/ACM International Conference on Computer Architecture (ISCA)*, 2016.
- [3] M. Bojarski, D. Del Testa, D. Dworakowski, B. Firner, B. Flepp, P. Goyal, L. D. Jackel, M. Monfort, U. Muller, J. Zhang *et al.*, “End to end learning for self-driving cars,” *arXiv preprint arXiv:1604.07316*, 2016.
- [4] Y. Chen, T. Luo, S. Liu, S. Zhang, L. He, J. Wang, L. Li, T. Chen, Z. Xu, N. Sun, and O. Temam, “Dadiannao: A machine-learning supercomputer,” in *Microarchitecture (MICRO), 2014 47th Annual IEEE/ACM International Symposium on*, Dec 2014, pp. 609–622.
- [5] M. Courbariaux, Y. Bengio, and J.-P. David, “BinaryConnect: Training Deep Neural Networks with binary weights during propagations,” *ArXiv e-prints*, Nov. 2015.
- [6] A. Delmas, P. Judd, S. Sharify, and A. Moshovos, “Dynamic stripes: Exploiting the dynamic precision requirements of activation values in neural networks,” *CoRR*, vol. abs/1706.00504, 2017. [Online]. Available: <http://arxiv.org/abs/1706.00504>
- [7] A. Delmas, S. Sharify, P. Judd, and A. Moshovos, “Tartan: Accelerating fully-connected and convolutional layers in deep learning networks by exploiting numerical precision variability,” *CoRR*, vol. abs/1707.09068, 2017. [Online]. Available: <http://arxiv.org/abs/1707.09068>
- [8] H. Esmailzadeh, E. Blem, R. St. Amant, K. Sankaralingam, and D. Burger, “Dark silicon and the end of multicore scaling,” in *Proceedings of the 38th Annual International Symposium on Computer Architecture*, ser. ISCA ’11. New York, NY, USA: ACM, 2011, pp. 365–376.
- [9] S. Han, X. Liu, H. Mao, J. Pu, A. Pedram, M. A. Horowitz, and W. J. Dally, “EIE: Efficient Inference Engine on Compressed Deep Neural Network,” *arXiv:1602.01528 [cs]*, Feb. 2016, arXiv: 1602.01528. [Online]. Available: <http://arxiv.org/abs/1602.01528>
- [10] F. N. Iandola, M. W. Moskewicz, K. Ashraf, S. Han, W. J. Dally, and K. Keutzer, “Squeezenet: Alexnet-level accuracy with 50x fewer parameters and <1mb model size,” *CoRR*, vol. abs/1602.07360, 2016. [Online]. Available: <http://arxiv.org/abs/1602.07360>
- [11] P. Judd, J. Albericio, T. Hetherington, T. Aamodt, N. Enright Jerger, and A. Moshovos, “Proteus: Exploiting numerical precision variability in deep neural networks,” in *Workshop On Approximate Computing (WAPCO)*, 2016.
- [12] P. Judd, J. Albericio, T. Hetherington, T. Aamodt, N. Enright Jerger, R. Urtasun, and A. Moshovos, “Reduced-Precision Strategies for Bounded Memory in Deep Neural Nets,” arXiv:1511.05236v4 [cs.LG], *arXiv.org*, 2015.
- [13] P. Judd, J. Albericio, T. Hetherington, T. Aamodt, and A. Moshovos, “Stripes: Bit-serial Deep Neural Network Computing,” in *Proceedings of the 49th Annual IEEE/ACM International Symposium on Microarchitecture*, ser. MICRO-49, 2016.
- [14] J. Kim, K. Hwang, and W. Sung, “X1000 real-time phoneme recognition VLSI using feed-forward deep neural networks,” in *2014 IEEE International Conference on Acoustics, Speech and Signal Processing (ICASSP)*, May 2014, pp. 7510–7514.
- [15] A. Parashar, M. Rhu, A. Mukkara, A. Puglielli, R. Venkatesan, B. Khailany, J. Emer, S. W. Keckler, and W. J. Dally, “Scnn: An accelerator for compressed-sparse convolutional neural networks,” in *Proceedings of the 44th Annual International Symposium on Computer Architecture*, ser. ISCA ’17. New York, NY, USA: ACM, 2017, pp. 27–40. [Online]. Available: <http://doi.acm.org/10.1145/3079856.3080254>
- [16] S. Sharify, A. D. Lascorz, P. Judd, and A. Moshovos, “Loom: Exploiting weight and activation precisions to accelerate convolutional neural networks,” *CoRR*, vol. abs/1706.07853, 2017. [Online]. Available: <http://arxiv.org/abs/1706.07853>
- [17] P. Warden, “Low-precision matrix multiplication,” <https://petewarden.com>, 2016.
- [18] M. Zhu and S. Gupta, “To prune, or not to prune: exploring the efficacy of pruning for model compression,” *ArXiv e-prints*, Oct. 2017.

## Bios

Andreas Moshovos completed his PhD studies in Computer Science at the University of Wisconsin-Madison. He is currently a Professor at the Electrical and Computer Engineering Department of the University of Toronto. His research interests are in architecting highly-efficient and high-performance computing hardware. He is a senior member of the IEEE and the ACM.

Jorge Albericio obtained his PhD degree in Systems Engineering and Computing from the University of Zaragoza in 2013. He was a postdoctoral fellow at the University of Toronto from 2013 to 2016 where he worked on branch prediction, approximate computing, and hardware accelerators for machine learning. He is a Senior Deep Learning Architect at NVIDIA. He is a member of the IEEE.

Patrick Judd is a 4th year PhD Candidate at the University of Toronto. His research interests include computer architecture, machine learning, and approximate computing. His research focuses on the design of hardware accelerators for deep neural networks that exploit approximation for improved performance and energy efficiency. Patrick also received his MASc and BASc from the University of Toronto. He is a student member of the IEEE.

Alberto Delmàs is in his third year at the University of Toronto as a Ph.D. student, focusing in hardware design for machine learning accelerators. His research interests include computer architecture, deep learning, and embedded and reconfigurable systems. He graduated in Computer Engineering from University of Zaragoza in 2014. He is a student member of the IEEE.



Sayeh Sharify received her B.Sc. degree in Computer Engineering from Sharif University of Technology in 2013, and her M.A.Sc. degree in Electrical Engineering from University of Toronto in 2015, where she is currently a third year Ph.D. student. Her research interests include computer architecture, machine learning, embedded systems, and reconfigurable computing. She is currently working on designing hardware accelerators for machine learning algorithms. She is a student member of the IEEE and the ACM.

Taylor Hetherington is in the final year of his PhD in Computer Engineering at the University of British Columbia and is currently working at Oracle Labs. He received his B.A.Sc. in Computer Engineering from the University of British Columbia in 2011. His research interests include computer architecture, specifically general-purpose graphics processing units and machine learning accelerators, and system software. He is a student member of the

IEEE.

Tor Aamodt received his PhD in electrical and computer engineering from the University of Toronto in 2006. He is currently a Professor in the Department of Electrical and Computer Engineering at the University of British Columbia. His research interests include architecture of general-purpose graphics processor units and machine learning accelerators. He is a member of the IEEE and ACM.

Natalie Enright Jerger received her PhD degree in electrical engineering from the University of Wisconsin-Madison in 2008. She is currently the Percy Edward Hart Professor of Electrical and Computer Engineering at the University of Toronto. Her research interests include computer architecture, approximate computing, interconnection networks and hardware acceleration of machine learning. She is a senior member of the IEEE and ACM.